J Mater Sci: Mater Med (2011) 22:165–174
DOI 10.1007/s10856-010-4174-6

# Enhanced osteogenic differentiation of cord blood-derived unrestricted somatic stem cells on electrospun nanofibers

**Ehsan Seyedjafari · Masoud Soleimani · Nasser Ghaemi · Mohammad Nabi Sarbolouki**

Received: 6 June 2010 / Accepted: 21 October 2010 / Published online: 11 November 2010


**Abstract** A new stem cell-scaffold construct based on poly-L-lactide (PLLA) nanofibers grafted with collagen (PLLA-COL) and cord blood-derived unrestricted somatic stem cells (USSC) were proposed to hold promising characteristics for bone tissue engineering. Fabricated nanofibers were characterized using SEM, ATR-FTIR, tensile and contact angle measurements. The capacity of PLLA, plasma-treated PLLA (PLLA-pl) and PLLA-COL scaffolds to support proliferation and osteogenic differentiation of USSC was evaluated using MTT assay and common osteogenic markers such as alkaline phosphatase (ALP) activity, calcium mineral deposition and bone-related genes. All three scaffolds showed nanofibrous and porous structure with suitable physical characteristics. Higher proliferation and viability of USSC was observed on PLLA-COL nanofibers compared to control surfaces. In osteogenic medium, ALP activity and calcium deposition exhibited the highest values on PLLA-COL scaffolds on days 7 and 14. These markers were also greater on PLLA and PLLA-pl compared to TCPS. Higher levels of collagen I, osteonectin and bone morphogenetic protein-2 were detected on PLLA-COL compared to PLLA and PLLA-pl. Runx2 and osteocalcin were also expressed continuously on all scaffolds during induction. These observations suggested the enhanced proliferation and osteogenic differentiation of USSC on PLLA-COL nanofiber scaffolds and introduced a new combination of stem cell-scaffold constructs with desired characteristics for application in bone tissue engineering.

Mohammad Nabi Sarbolouki deceased in 2009.

E. Seyedjafari · N. Ghaemi
Department of Biotechnology, College of Science, University of Tehran, Tehran, Iran

E. Seyedjafari
Stem Cell Biology Department, Stem Cell Technology Research Center, Tehran, Iran

M. Soleimani (✉)
Hematology Department, Faculty of Medical Science, Tarbiat Modares University, P.O. Box 14115-111, Tehran, Iran
e-mail: soleim_m@modares.ac.ir
URL: http://www.stemcellstech.com

N. Ghaemi
School of Chemistry, College of Science, University of Tehran, Tehran, Iran

M. N. Sarbolouki
Institute of Biophysics and Biochemistry, University of Tehran, Tehran, Iran

## 1 Introduction

Natural extracellular matrix (ECM) is a highly complex structure and is composed of various proteins with nanoscale dimensions which support cell adhesion, proliferation and differentiation [1]. In bone ECM, collagen type I fibrils are the major organic components and serve as a template upon which minerals like calcium phosphates are deposited. This organized composition contributes to provide mechanical and biological properties of bone and may play an important role in the maturation of bone stem cells and progenitors during regeneration and reconstruction after injury or damage [2, 3].

Mimicking the biomechanical and biological structure of ECM is an effective strategy to design and develop scaffolds in the field of tissue engineering [4]. Nanofibrous

scaffolds can ideally mimic the physical structure of ECM and can be fabricated via a few procedures such as phase separation, self-assembly and electrospinning. Among them, electrospinning is the most widely used method because of its simplicity, cost-effectiveness and potential to apply a wide range of polymers for mass production of nanofibers [5]. Electrospun nanofibers are highly favored as tissue-engineered scaffolds because in addition to ECM-mimicking, they can be surface modified to improve their biocompatibility and bioactivity [6, 7].

In recent years, stem cell-based tissue engineering has received much attention because of the unique characteristics of stem cells such as multi-potency, self-renewal and high potential for ex vivo expansion. In this approach, stem cells derived from different sources in embryonic, neonatal or adult stages, are incorporated with appropriate biomaterials and their potential for tissue engineering are investigated in vitro [8]. Using this idea, many efforts have been performed to develop efficient combination of nanofibers and stem cells for application in bone tissue engineering. Electrospun nanofibers fabricated from various polymers in combination with embryonic, mesenchymal and adipose-derived stem cells have been shown to have potential application in bone tissue engineering [9–13].

Unrestricted somatic stem cells have been recently isolated from human umbilical cord blood (UCB) and have interesting characteristics for application in tissue engineering [14]. They have the potential to differentiate into three germ layers and remain undifferentiated without transformation after long-term ex vivo expansion. Compared to bone marrow derived mesenchymal stem cells (BM-MSC), isolation of unrestricted somatic stem cells (USSC) is non-invasive and is performed more easily from UCB which is discarded after child birth. They also have better growth kinetics with a broader life-span up to more than 20 passages and their immunogenicity and ethical issues is less controversial [15–17]. Such proliferative and multipotent stem cells are a promising and interesting source for the future of cell-based therapies and regenerative medicine.

In a previous study, we showed that PCL nanofibers could support in vitro differentiation of USSC toward hepatocyte-like cells [18]. Further, our findings suggested that USSC had the capacity to attach, proliferate and infiltrate on collagen-grafted nanofibers prepared from polyethersulfone [19]. To the best of our knowledge, osteogenic behavior of USSC on nanofibers has been never studied before. Therefore, in the present study we investigated the capacity of USSC in combination with pure and collagen-grafted PLLA nanofibers for application in bone tissue engineering.

## 2 Materials and methods

### 2.1 Isolation and expansion of USSC

Collection, isolation and culture of human USSC were performed as described previously [19]. Briefly, cord blood was collected from the umbilical cord vein with informed consent of the mother. Then mononuclear cell fraction was separated by density centrifugation over a Ficoll-Hypaque gradient (Amersham Pharmacia, NJ, USA; d = 1.077 g/ml) and further was cultured in low glucose DMEM (GIBCO-BRL, Grand Island, NY, USA) supplemented with 30% FBS (Gibco), dexamethasone ($10^{-7}$ M; Sigma–Aldrich, MO, USA), L-glutamine (2 mM; Gibco), penicillin (100 U/ml; Gibco) and streptomycin (0.1 mg/ml; Gibco). After almost 2 weeks, USSC colonies were appeared, then the cells were detached with 0.25% Trypsin–EDTA (Gibco) and were cultured in a humidified atmosphere of 95% air with 5% $CO_2$ at 37°C and DMEM with 10% FBS. Passage 2 (P2) cells were used for this study. For osteogenic differentiation, USSC were cultured in DMEM supplemented with 10% FBS, 10 nM dexamethasone, 0.2 mM ascorbic acid 2-phosphate, and 10 mM $\beta$-glycerophosphate (all from Sigma).

### 2.2 Scaffold preparation

Nanofibrous PLLA scaffolds were prepared via electrospinning as previously performed in our Lab [20]. Briefly, a 12% solution of PLLA (sigma) in dichloromethane (Merck, Germany) was placed in a 5 ml syringe. An extension tube connected the syringe to a 21-gauge needle which was placed in a 15 cm distance from a steel cylinder collector. The solution fed through the tube into the needle by a syringe pump. Application of a 20 kV-voltage between the needle and collector, forced the solution droplet to leave the needle and collect on the cylinder as fibers with nano-sized diameters.

### 2.3 Collagen grafting

Collagen I solution (Nutacon BV, the Netherlands) was grafted onto the surface of PLLA nanofibers via chemical cross-linking after surface plasma treatment by low frequency plasma generator of 44 GHz frequency with a cylindrical quartz reactor (Diener Electronics, Germany). Pure oxygen was introduced into the reaction chamber at 0.4 mbar pressure and then the glow discharge was ignited for 5 min. For collagen grafting, plasma-treated sheets were cut into 1.5 cm diameter punches and immersed in EDC/NHS (Merck) solution (5 mg/ml) for 12 h. A 1 mg/ml collagen I solution was used to immerse scaffolds

overnight. The scaffolds were then rinsed with distilled water. All of the further experiments were performed on PLLA, plasma-treated PLLA (PLLA-pl) and collagen-grafted PLLA (PLLA-COL).

### 2.4 Cell seeding

Prior to cell seeding, circular scaffolds were immersed overnight in the following solutions: (1) 70% ethanol for sterilization, (2) penicillin, streptomycin, and amphotericin B to prevent from yeast growth, and (3) culture medium to ensure sterilization and enhance cell attachment after seeding. USSC were trypsinized and seeded onto the circular scaffolds at an initial cell density of $5 \times 10^3$ $cm^{-1}$. After reaching 70% confluence which was estimated by DAPI staining, culture medium was replaced with osteogenic medium which was changed every 2–3 days for 2 weeks.

### 2.5 Scanning electron microscopy

The surface morphology of scaffolds was characterized using a scanning electron microscope (SEM, Philips XL30, the Netherlands) after specimens were coated with platinum using a sputter coater. The fiber diameter was determined from SEM images using image analysis software (imageJ, NIH, USA). Three images from each sample were selected and the diameter of 50 individual fibers was measured from each SEM image. Morphology of USSC on the scaffolds during osteogenic differentiation was also investigated by SEM. The cell-loaded scaffolds were rinsed with PBS after 7 and 14 days of osteogenic differentiation and fixed in glutaraldehyde 2.5% for 1 h. For dehydrating, the scaffolds were placed in a series of gradient of alcohol concentration and then dried.

### 2.6 Contact angle measurement

To study the wettability of the nanofiber surface after surface treatment, water contact angle was measured by the sessile drop method with a G10 Kruss contact angle goniometer at room temperature. A water droplet is placed on the scaffold surface and contact angle was measured after 10 s.

### 2.7 ATR-FTIR spectroscopy

Collagen grafting was investigated by FTIR-ATR. The spectra were recorded using an Equinox 55 spectrometer (*Bruker* Optics, Germany) equipped with a DTGS detector and a diamond ATR crystal.

### 2.8 Mechanical properties

The tensile properties were performed on the nanofibrous webs using Galdabini testing equipment. Prepared scaffolds were cut into 10 mm × 60 mm × 0.11 mm specimens and tensile test was conducted at 50 mm/min crosshead speed at room temperature.

### 2.9 MTT assay

The proliferation of USSC on different scaffolds was evaluated via MTT assay. Sterilized nanofibrous membranes were placed in a 24-well culture plate, seeded with a cell density of $8 \times 10^3$ cells per $cm^2$, and incubated at 37°C, 5% $CO_2$. After 1, 3, 5 and 7 days of cell seeding, 50 µl of MTT solution (5 mg/ml in DMEM) was added to each well ($n = 4$). For conversion of MTT to formazan crystals by mitochondrial dehydrogenases of living cells, the plate was incubated at 37°C for 3.5 h. For dissolution of the dark-blue intracellular formazan, the supernatant was removed and constant amount of an appropriate solvent was added. The optical density was read spectrophotometrically at a wavelength of 570 nm. The same procedure was performed for cultured cells in tissue culture polystyrene (TCPS) as control.

### 2.10 Real-time RT-PCR

To quantify the difference between the mRNA levels of osteogenic markers, gene expression in USSC on scaffolds was analyzed using real-time RT-PCR. Total RNA was extracted and random hexamer primed cDNA synthesis was carried out using Revert Aid first strand cDNA synthesis kit (Fermentas, Burlington, Canada). cDNA was used for 40 cycle PCR in Rotor-gene Q real-time analyzer (Corbett, Australia). Real-time PCR was performed using Maxima™ SYBR Green/ROX qPCR Master Mix (Fermentas) followed by melting curve analysis to confirm PCR specificity. Each reaction was repeated three times and threshold cycle average was used for data analysis by Rotor-gene Q software (Corbett). Genes and related specific primers are illustrated in Table 1. Relative expression was quantified using ΔΔCt method. Target genes were normalized against GAPDH and calibrated to USSC P2.

### 2.11 Alkaline phosphatase (ALP) activity

For ALP activity measurement, total protein of cells on TCPS and scaffolds was extracted using 200 µl RIPA buffer. The lysate was then centrifuged at 14,000×*g* at

**Table 1** Primers used in real-time RT-PCR

| Gene | Primer sequence (5′→3′) | Product length (bp) |
|---|---|---|
| GAPDH | F: CTCTCTGCTCCTCCTGTTCG | 114 |
| | R: ACGACCAAATCCGTTGACTC | |
| ALP | F: GCACCTGCCTTACTAACTC | 162 |
| | R: AGACACCCATCCCATCTC | |
| Collagen I | F: TGGAGCAAGAGGCGAGAG | 122 |
| | R: CACCAGCATCACCCTTAGC | |
| Runx2 | F: GCCTTCAAGGTGGTAGCCC | 67 |
| | R: CGTTACCCGCCATGACAGTA | |
| Osteonectin | F: AGGTATCTGTGGGAGCTAATC | 224 |
| | R: ATTGCTGCACACCTTCTC | |
| Osteocalcin | F: GCAAAGGTGCAGCCTTTGTG | 80 |
| | R: GGCTCCCAGCCATTGATACAG | |
| BMP2 | F: TGCGGTCTCCTAAAGGTC | 186 |
| | R: AACTCGAACTCGCTCAGG | |

4°C for 15 min to sediment cell debris. Supernatant was collected and ALP activity was measured with ALP assay kit (Parsazmun, Tehran, Iran) using *p*-nitrophenyl phosphate (*p*-NPP) as substrate and alkaline phosphatase provided in the kit as a standard. The activity of enzyme (IU) was normalized against total DNA (μg) which was quantified using Quant-iT Picogreen (Invitrogen, Eugene, OR, USA). A standard curve of fluorescence intensity versus DNA concentration was first generated before use. The fluorescence intensity was determined at 480 nm excitation and 520 nm emission using a fluorometer.

### 2.12 Calcium content assay

During osteogenic differentiation of USSC, the amount of calcium deposited on different scaffolds and TCPS, was measured using cresolphthalein complexone method. Calcium extraction was performed by homogenization of the scaffolds in 0.6 N HCL (Merck) followed by shaking for 4 h at 4°C. Optical density was measured at 570 nm after the addition of the reagent to calcium solutions. Calcium content was obtained from the standard curve of OD versus a serial dilution of calcium concentrations.

### 2.13 Statistical analysis

All experiments were conducted at least 3 times. Data are expressed as mean ± SD. One-way analysis of variance (ANOVA) was used to compare results. A *P*-value of less than 0.05 was considered statistically significant.

## 3 Results

### 3.1 Characterization of scaffolds

PLLA electrospun nanofibers were porous, beads-free and had a uniform and smooth morphology (Fig. 1a, d) with an average diameter of 838 ± 92 nm, tensile strength of 1.91 ± 0.31 MPa and elongation at break of 82.1 ± 6.3%. After surface modification, it was obvious that plasma treatment and collagen I grafting did not affect the morphology and average diameter of nanofibers (Fig. 1). There was also no significant difference between tensile properties before and after modification (data not shown). Collagen grafting on the surface of nanofibers was investigated via ATR-FTIR spectroscopy (Fig. 2). PLLA nanofibers showed strong characteristic peaks at 1749 $cm^{-1}$ for C=O group and at 1083 for C–O stretching. Vibration of C–H band was also characterized with peaks near 3000. Existence of collagen was confirmed through the Amide I and II bands which were detected at 1633 and 1531 $cm^{-1}$. Contact angle of PLLA nanofibers also decreased from 112° to a zero value after surface treatment.

### 3.2 Biocompatibility of nanofibers

Biocompatibility of scaffolds was investigated via MTT assay which revealed the proliferation rate and viability of USSC on PLLA, PLLA-pl and PLLA-COL nanofibers (Fig. 3). With an equal initial cell density on day 1, no significant difference was observed between the rate of proliferation on PLLA-COL and TCPS until day 5. On day 7, the highest cellularity was measured on PLLA-COL compared to other groups. The cells had also a higher rate of proliferation on PLLA-pl compared to PLLA. On days 7 and 14 of osteogenic culture, the morphology of USSC on electrospun scaffolds was also investigated via SEM. USSC showed a spreading and typical morphology on day 7 and 14 on PLLA, PLLA-pl and PLLA-COL nanofibers (Fig. 4).

### 3.3 Assessment of osteogenic markers

#### *3.3.1 ALP activity and mineralization*

The pattern of ALP activity during osteogenic differentiation of USSC on scaffolds and TCPS was similar but exhibited different values (Fig. 5a) Increase in ALP activity was detected from day 3 to 7 followed by a decrease to day 14. On days 7 and 14 of osteogenic differentiation, the highest ALP activity was measured on PLLA-COL compared to other groups and there was no significant difference between ALP activity on PLLA and PLLA-pl. Higher values of ALP activity was also measured

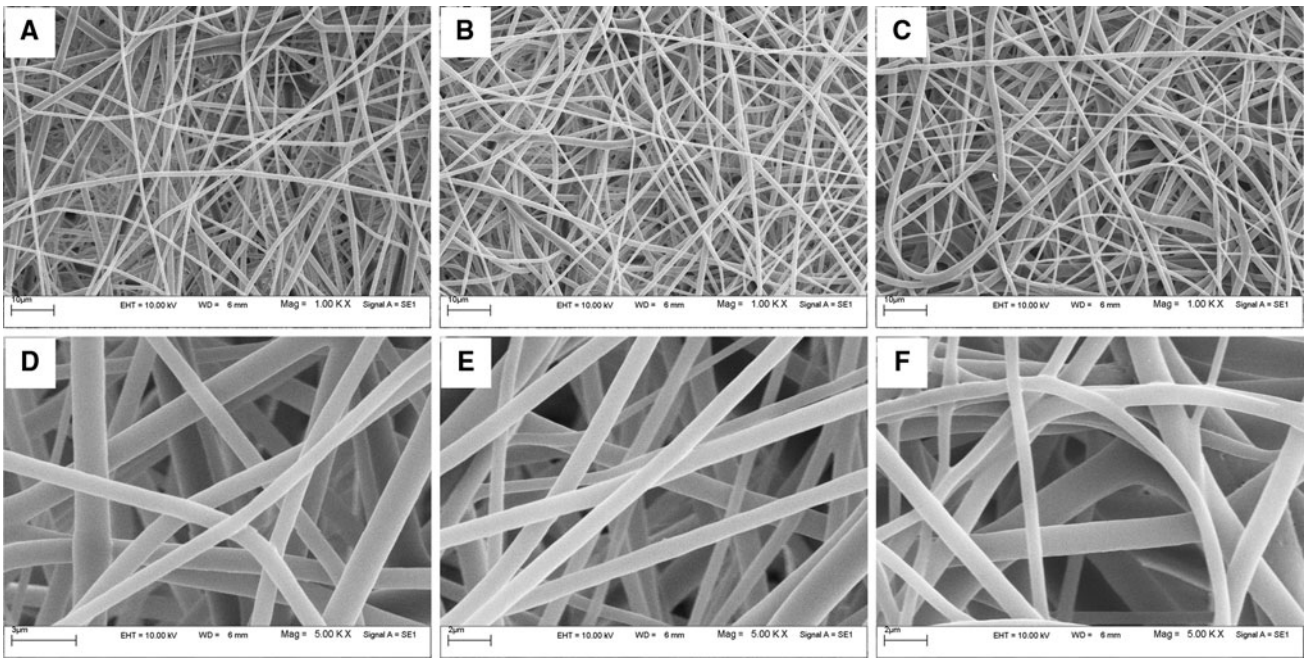


**Fig. 1** Morphology of fabricated scaffolds, PLLA (**a**, **d**), PLLA-pl (**b**, **e**) and PLLA-COL (**c**, **f**) nanofibers at 1,000× (**a**–**c**) and 5,000× (**d**–**f**)

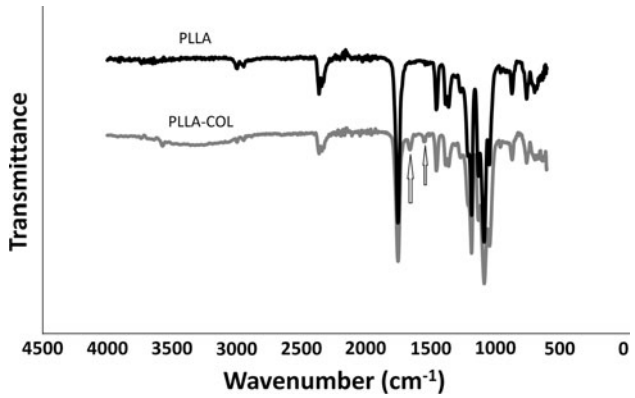


**Fig. 2** ATR-FTIR spectra of PLLA and PLLA-COL

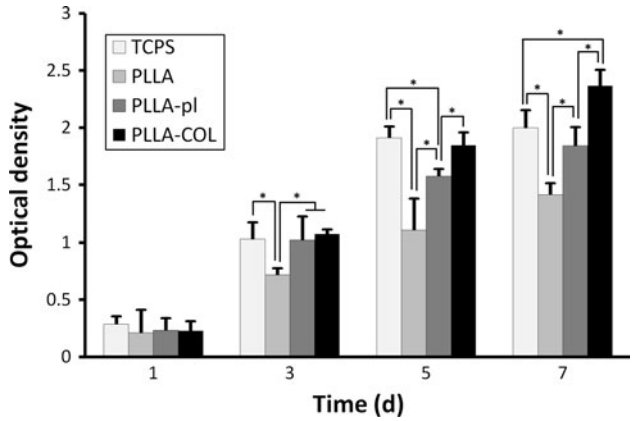


**Fig. 3** Proliferation of USSC on scaffolds and TCPS during a 7 day culture period, *asterisk* shows significant difference with $P < 0.05$

in the cells on PLLA and PLLA-pl compared to TCPS on day 7.

Mineralization as the late marker of differentiation toward osteoblasts was also assessed. Significant increasing of calcium depositions on scaffolds and control was observed during culture under osteogenic medium (Fig. 5b). Higher amount of deposited calcium was measured on PLLA-COL compared to PLLA, PLLA-pl and TCPS on day 7 and 14. The mineralization was also higher on PLLA and PLLA-pl compared to TCPS on day 14 and there was no significant difference between the amounts of mineralized calcium on these scaffolds. Huge calcium deposits on PLLA-COL nanofibers were observed on day 14 of differentiation. Porous structure of mineral depositions including aggregated globular nodules with collagen bundles is clearly obvious in higher magnifications (Fig. 6).

### 3.3.2 *Gene expression analysis*

The mRNA levels of six osteoblast-related genes were studied in USSC on electrospun nanofibers (Fig. 7). From a global aspect, in comparison to PLLA and PLLA-pl scaffolds, USSC on PLLA-COL expressed higher levels of transcripts. On all scaffolds, expression of ALP reached a peak on day 3 followed by a down-regulation on days 7 and 14. Collagen I was down-regulated continuously during osteogenic induction and higher levels of collagen I transcripts was observed on PLLA-COL nanofibers on day 3 and decreased to a value of that on PLLA and PLLA-pl on

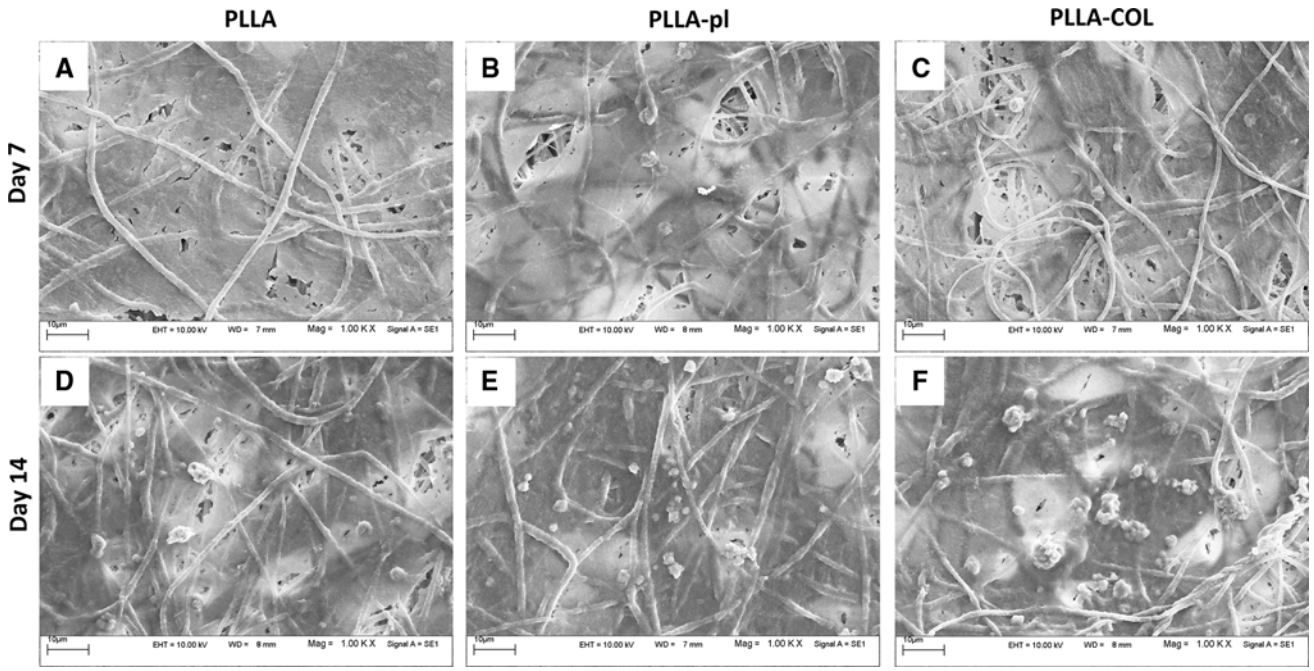


**Fig. 4** Morphology of USSC during osteogenic differentiation on nanofibrous PLLA (**a**, **d**), PLLA-pl (**b**, **e**) and PLLA-COL (**c**, **f**) on days 7 (**a**–**c**) and 14 (**d**–**f**)

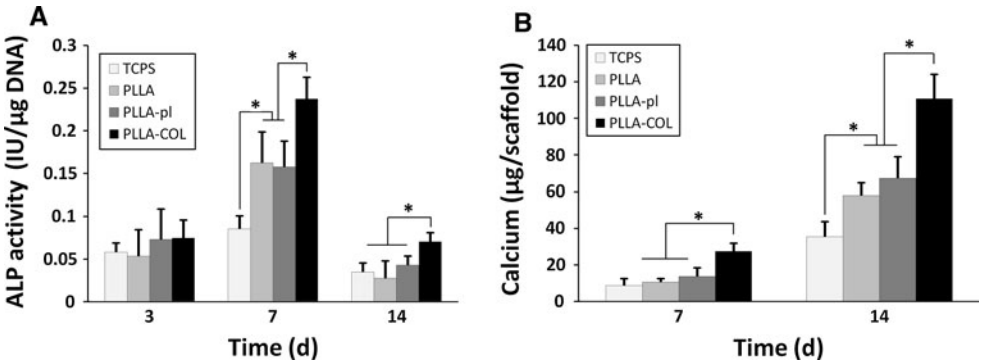


**Fig. 5** ALP activity (**a**) and calcium content (**b**) of USSC on scaffolds during osteogenic differentiation, *asterisk* show significant difference with $P < 0.05$

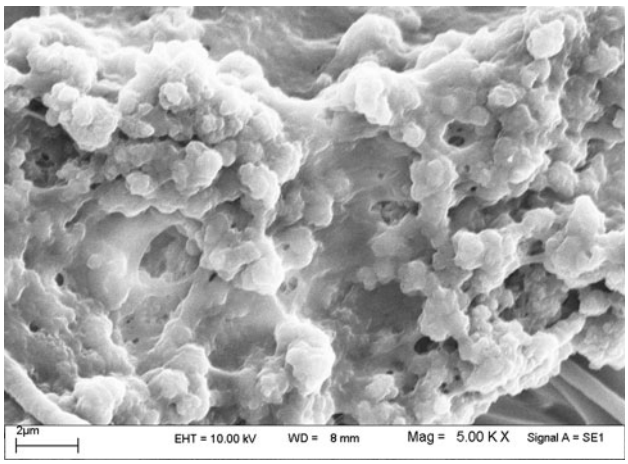


**Fig. 6** Mineral deposition of USSC after 14 of osteogenic differentiation

day 7 and 14. Runx2 was expressed continuously during culture on all scaffolds with no significant difference. Significant higher values of osteonectin transcripts were detected in all time points on PLLA-COL compared to PLLA and PLLA-pl. In addition, osteonectin was expressed in a higher amount on day 7 on PLLA-pl compared to PLLA. On day 14, this gene was down-regulated on all scaffolds. There was no significant difference between the expression of osteocalcin on all scaffolds during culture except day 7 on which this gene had higher levels of transcripts on PLLA-COL and PLLA-pl compared to PLLA. The (bone morphogenetic protein-2) BMP-2 expression increased continuously on scaffolds during time. This gene was expressed in a higher amount on PLLA-COL compared to PLLA and PLLA-pl on day 7 and 14.

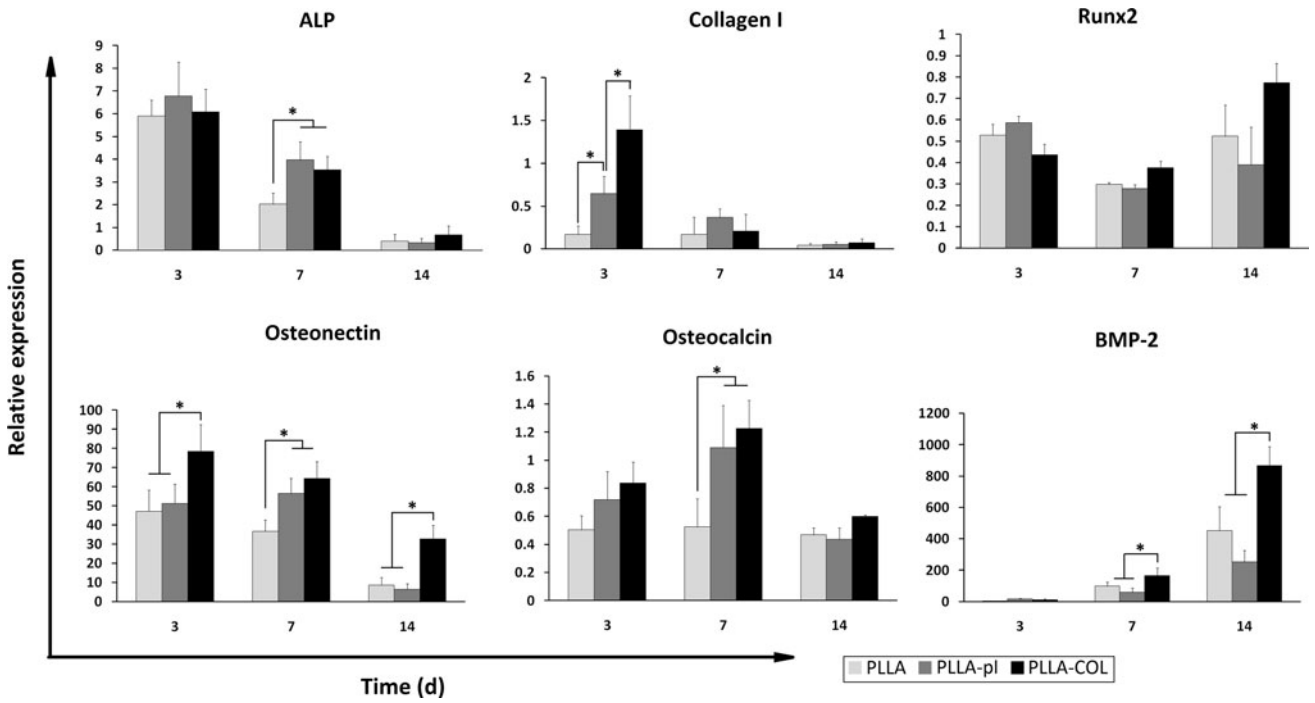


**Fig. 7** Relative expression of ALP, Collagen I, Runx2, Osteonectin, Osteocalcin and BMP-2 on days 3, 7 and 14 in USSC on scaffolds during osteogenic differentiation, *asterisk* shows significant difference with $P < 0.05$

## 4 Discussion

In the present study for the first time, we investigated the osteogenic differentiation of USSC on electrospun nanofibrous scaffolds. Recently introduced USSC have shown promising characteristics for application in cell-based therapies and tissue engineering [21–23]. Electrospun nanofibers alone or surface modified with bioactive molecules have attracted much attention in the field of tissue engineering mainly because of their ECM-mimicking structure [4]. We postulated that USSC-nanofibers construct under osteogenic induction would give rise to a potential scaffold for application in bone tissue engineering.

PLLA blended with collagen has been electrospun to nanofibers in a few recent reports [24, 25]. In these studies, PLLA-COL nanofibers have shown similar biocompatibility in comparison to unmodified PLLA. Collagen I serve as the major protein component of bone ECM and is mineralized during bone formation and regeneration. Collagen I exist as nano-sized fibrils and play an important role to provide physical and chemical clues to maintain bone function [26]. Surface grafting of PLLA nanofibers with collagen I will lead to a tissue-engineered scaffold which benefit from both nano scale structure of PLLA fibers and bioactivity of collagen I. Ideally, physical properties of PLLA scaffold such as porosity, fiber diameter and tensile strength were not significantly changed after modification. Data from MTT assay showed that the biocompatibility of PLLA nanofibers increased after plasma treatment and collagen grafting. In another word, all scaffolds showed the capacity to support adhesion and proliferation of USSC with an enhanced viability on PLLA-COL scaffolds. This can be explained by the bioactivity of collagen which provides natural adhesion sites for cells to attach and proliferate [27]. The higher rate of cell proliferation on PLLA-pl and PLLA-COL scaffolds compared to PLLA can be also explained by the increased hydrophilicity which its effect on cell attachment and proliferation on biomaterials have been well established [28, 29]. Biocompatibility of nanofibers was also confirmed qualitatively by flattened and spreading morphology of USSC under inductive culture.

Beside the biocompatibility and appropriate physical characteristics of biomaterials, the capacity to support osteogenic differentiation of stem cells is of major importance in stem cell-scaffold approach for bone tissue engineering. To assess this capacity, osteo-lineage related markers need to be monitored during osteogenic induction of stem cells.

ALP has a critical role in bone matrix mineralization through cleavage of phosphate group and its elevated activity is observed before the initiation of calcium minerals [30]. Therefore, increase in the ALP activity is considered as an early-stage marker of osteogenic differentiation of stem cells which was reported previously in MSC [31] and USSC [14]. In our study a similar trend for ALP activity was observed on scaffolds and TCPS; an increase to day 7

followed by a decrease in ALP activity to day 14. This pattern was consistent with other reports which have monitored ALP activity in USSC cultured on plastic surface under osteogenic induction [14, 32]. Higher ALP activity on PLLA-COL compared to PLLA and PLLA-pl on day 7, showed the effect of collagen I in early orientation of USSC toward osteo-lineage. In addition to ALP activity, calcium mineralization is also considered as a hallmark of osteoblast-like cells derived from stem cells under osteo-induction [33, 34]. Mineralization is naturally occurred through an orchestrated process during which osteo-progenitors derived osteoblasts force ionic calcium to deposit on the highly organized structure of collagen nanofibrillar network [35]. In addition to the increasing amount of calcium deposits on nanofibers and control during inductive culture, the role of collagen I in enhancement of osteogenic differentiation was confirmed from the high capacity of USSC on PLLA-COL nanofibers to mineralize extracellular calcium. Although PLLA and PLLA-pl nanofibers could not support the proliferation of USSC as well as TCPS, their higher mineralization and ALP activity suggested the role of nanofibrous structure in enhancement of osteogenic differentiation of USSC. There was also no significant difference between the ALP activity and mineralization on PLLA and PLLA-pl scaffolds. This is indicative that plasma treatment had no effect on the induction of USSC toward osteogenic lineage. The unique structure of mineral depositions formed on PLLA-COL nanofibers can suitably mimic the inorganic phase of natural bone. The choice of USSC over other stem cells for application in cell therapy and tissue engineering can be explained by their lower immunogenicity, ethical challenges and morbidity after isolation [15]. It has been shown that USSC had the potential for ectopic bone formation with higher mineralization values over than ESCs in rat muscle [36]. A recent report also studied the behavior and osteogenic differentiation of USSC on different kind of biomaterials [37]. In the present study, we showed that formation of bio-appetite along with bioactive nanofibers and osteoblast-like cells derived from USSC contribute to a potential stem cell-scaffold complex for bone tissue engineering.

Expression of osteoblast-related genes during osteogenic differentiation of stem cells, have been shown to exert a unique pattern and is helpful to understand the mechanism of bone regeneration [38]. This knowledge is essential for further contribution in design and development of efficient cell-scaffold constructs. Six bone-related genes from different stages of development of osteoblast-like cells were selected to study their regulation in USSC on scaffolds.

During osteogenic differentiation, the pattern of ALP transcripts showed that its expression peaked prior to the time in which ALP activity reached its maximum level on all scaffolds. Higher mineralization capacity of USSC on PLLA-COL nanofibers could be explained by their higher transcripts of osteogenic genes. Collagen I is the most abundant protein in bone matrix and its nanofibrillar structure provide a physical pattern for mineralization during bone formation [35]. Up-regulation of collagen I during osteogenic differentiation of MSC from different sources has been reported [39]. On the contrary, down-regulation of a set of ECM-related genes including collagen I was reported during osteogenic differentiation of adipose-tissue derived MSC. In our study, we also observed decreasing trend of collagen I expression in USSC under osteo-inductive culture. However, not only early down-regulation on PLLA and PLLA-pl but also higher levels of collagen I expression on PLLA-COL on day 3 showed the higher osteogenic capacity of USSC on PLLA-COL nanofibers. This higher capacity was further confirmed by results from expression of osteonectin and BMP-2.

Osteonectin is a phosphorylated glycoprotein which has a role in regulating the initiation and promotion of mineralization and crystal growth [40]. The role of osteonectin as an immediate-stage marker was confirmed based on the observed trend with higher expression on PLLA-COL compared to PLLA and PLLA-pl. BMP-2 is a well known osteogenic growth factor which has an important role in osteo-induction in vivo and in vitro [41]. USSC showed higher levels of BMP-2 mRNA on PLLA-COL on day 7 and 14. This may contribute to enhance the expression and secretion of BMP-2 in culture medium and accelerate osteogenic differentiation of USSC in a feed-back pattern. Osteocalcin contains three carboxyglutamic acid residues which bind $Ca^{2+}$ and regulate mineralization and remodeling [42]. This gene was expressed in higher amounts on PLLA-Col and PLLA-pl compared to PLLA on day 7. This is indicative that in addition to collagen, plasma treatment has affected the regulation of this gene. It is known that Runx2 [43] is involved in the initial orientation of progenitors toward osteoblasts and binds as a transcription factor to osteocalcin promoter. Runx2 was continuously expressed in USSC on all scaffolds and down-regulated on day 7. These findings could explain the initiator effect on orientation of USSC toward osteo-lineage.

Taking together, enhanced differentiation of USSC was observed on PLLA and PLLA-pl nanofibers. Although the plasma treatment influenced the expression of some genes during osteogenic differentiation, there was no significant difference between the ALP activity and mineralization on PLLA-pl compared with PLLA. In addition, the existence of collagen I on the surface of nanofibers promoted osteogenic differentiation of USSC. Higher osteogenic potential of USSC under inductive culture was proved using bone-related biochemical and genetic markers. Taking this into account, combination of USSC and collagen-grafted PLLA nanofibers showed promising potential for

application in the field of bone tissue engineering. Despite the fact that ECM-mimicking structure of electrospun scaffolds can improve the biological and osteogenic behavior of stem cells, the infiltration of cells into the scaffolds to form a three dimensional architecture is essential for an efficient tissue-engineered construct. As shown in this study, USSC formed a monolayer of osteoblast-like cells after a 14 days culture on nanofibrous scaffolds under osteogenic induction. This may limit the application of stem cell-electrospun scaffold in tissue engineering. Different approaches and strategies have been used by researchers to address this issue. However, an ideal 3D structure of nanofibers incorporated with cells has not been achieved yet. Our future works will concern the improvement of stem cell infiltration via fine tuning of electrospinning parameters or modification of nanofibers with appropriate bioactive molecules and signals.

## 5 Conclusions

Due to a large amount of graft substitutes needed for a variety of bone injuries, effective scaffolds alone or incorporated with appropriate cells need to be developed. In this study, nanofibrous structure of PLLA and PLLA-pl supported the proliferation and promoted the osteogenic differentiation of USSC. In addition, greater viability and higher values of osteogenic markers such as ALP activity, calcium content and bone-related gene expression was observed in USSC on PLLA-COL. In another word, collagen-grafted PLLA nanofibers benefited simultaneously from their nanofibrous structure and bioactivity to enhance in vitro bone formation resulted from osteogenic differentiation of USSC. Further studies should contribute to in vivo evaluation of USSC-PLLA-COL constructs as a new graft substitute for bone tissue engineering.

## References


1. Daley WP, Peters SB, Larsen M. Extracellular matrix dynamics in development and regenerative medicine. J Cell Sci. 2008;121:255–64.
2. Fratzl P, Gupta H, Paschalis E, Roschger P. Structure and mechanical quality of the collagen–mineral nano-composite in bone. J Mater Chem. 2004;14:2115–23.
3. Datta N, Holtorf HL, Sikavitsas VI, Jansen JA, Mikos AG. Effect of bone extracellular matrix synthesized in vitro on the osteoblastic differentiation of marrow stromal cells. Biomaterials. 2005;26:971–7.
4. Ma Z, Kotaki M, Inai R, Ramakrishna S. Potential of nanofiber matrix as tissue-engineering scaffolds. Tissue Eng. 2005;11:101–9.
5. Huang Z, Zhang Y, Kotaki M, Ramakrishna S. A review on polymer nanofibers by electrospinning and their applications in nanocomposites. Composit Sci Technol. 2003;63:2223–53.
6. Park K, Ju Y, Son J, Ahn K, Han D. Surface modification of biodegradable electrospun nanofiber scaffolds and their interaction with fibroblasts. J Biomater Sci Polym Ed. 2007;18:369–82.
7. Li W, Guo Y, Wang H, Shi D, Liang C, Ye Z, et al. Electrospun nanofibers immobilized with collagen for neural stem cells culture. J Mater Sci Mater Med. 2008;19:847–54.
8. Bianco P, Robey PG. Stem cells in tissue engineering. Nature. 2001;414:118–21.
9. Smith LA, Liu X, Hu J, Wang P, Ma PX. Enhancing osteogenic differentiation of mouse embryonic stem cells by nanofibers. Tissue Eng Part A. 2009;15:1855–64.
10. Mohammadi Y, Soleimani M, Fallahi-Sichani M, Gazme A, Haddadi-Asl V, Arefian E, et al. Nanofibrous poly (epsilon-caprolactone)/poly (vinyl alcohol)/chitosan hybrid scaffolds for bone tissue engineering using mesenchymal stem cells. Int J Artif Organs. 2007;30:204.
11. Yoshimoto H, Shin YM, Terai H, Vacanti JP. A biodegradable nanofiber scaffold by electrospinning and its potential for bone tissue engineering. Biomaterials. 2003;24:2077–82.
12. Sefcik L, Neal R, Kaszuba S, Parker A, Katz A, Ogle R, et al. Collagen nanofibres are a biomimetic substrate for the serum-free osteogenic differentiation of human adipose stem cells. J Tissue Eng Regen Med. 2008;2:210.
13. Schofer MD, Boudriot U, Bockelmann S, Walz A, Wendorff JH, Greiner A, et al. Effect of direct RGD incorporation in PLLA nanofibers on growth and osteogenic differentiation of human mesenchymal stem cells. J Mater Sci Mater Med. 2009;20:1535–40.
14. Kogler G, Sensken S, Airey JA, Trapp T, Muschen M, Feldhahn N, et al. A new human somatic stem cell from placental cord blood with intrinsic pluripotent differentiation potential. J Exp Med. 2004;200:123–35.
15. Kögler G. The Unrestricted Somatic Stem Cell (USSC) From Cord Blood For Regenerative Medicine. In: Meyer UMT, Handschel J, Wiesmann HP, editors. Fundamentals of tissue engineering and regenerative medicine. Heidelberg: Springer; 2009. p. 167–76.
16. Sensken S, Waclawczyk S, Knaupp AS, Trapp T, Enczmann J, Wernet P, et al. In vitro differentiation of human cord blood-derived unrestricted somatic stem cells towards an endodermal pathway. Cytotherapy. 2007;9:362–78.
17. Fallahi-Sichani M, Soleimani M, Najafi S, Kiani J, Arefian E, Atashi A. In vitro differentiation of cord blood unrestricted somatic stem cells expressing dopamine-associated genes into neuron-like cells. Cell Biol Int. 2007;31:299–303.
18. Hashemi SM, Soleimani M, Zargarian SS, Haddadi-Asl V, Ahmadbeigi N, Soudi S, et al. In vitro differentiation of human cord blood-derived unrestricted somatic stem cells into hepatocyte-like cells on poly(epsilon-caprolactone) nanofiber scaffolds. Cells Tissues Organs. 2009;190:135–49.
19. Shabani I, Haddadi-Asl V, Seyedjafari E, Babaeijandaghi F, Soleimani M. Improved infiltration of stem cells on electrospun nanofibers. Biochem Biophys Res Commun. 2009;382:129–33.
20. Babaeijandaghi F, Shabani I, Seyedjafari E, Naraghi Z, Vasei M, Haddadi-Asl V, et al. Accelerated epidermal regeneration and improved dermal reconstruction achieved by polyethersulfone nanofibers. Tissue Eng Part A. 2010. doi:10.1089/ten.tea.2009.0829.
21. Degistirici Ö, Jäger M, Knipper A. Applicability of cord blood-derived unrestricted somatic stem cells in tissue engineering concepts. Cell Prolif. 2008;41:421–40.
22. Iwasaki H, Kawamoto A, Willwerth C, Horii M, Oyamada A, Akimaru H, et al. Therapeutic potential of unrestricted somatic stem cells isolated from placental cord blood for cardiac repair post myocardial infarction. Arterioscler Thromb Vasc Biol. 2009;29:1830–5.

23. Ghodsizad A, Niehaus M, Kogler G, Martin U, Wernet P, Bara C, et al. Transplanted human cord blood-derived unrestricted somatic stem cells improve left-ventricular function and prevent left-ventricular dilation and scar formation after acute myocardial infarction. Heart. 2009;95:27–35.
24. Ngiam M, Liao S, Patil A, Cheng Z, Yang F, Gubler M, et al. Fabrication of mineralized polymeric nanofibrous composites for bone graft materials. Tissue Eng Part A. 2008;15:535–46.
25. Chiu JB, Liu C, Hsiao BS, Chu B, Hadjiargyrou M. Functionalization of poly(L-lactide) nanofibrous scaffolds with bioactive collagen molecules. J Biomed Mater Res A. 2007;83:1117–27.
26. Weiner S, Wagner H. The material bone: structure-mechanical function relations. Annu Rev Mater Sci. 1998;28:271–98.
27. Chevallay B, Herbage D. Collagen-based biomaterials as 3D scaffold for cell cultures: applications for tissue engineering and gene therapy. Med Biol Eng Comput. 2000;38:211–8.
28. Kim C, Khil M, Kim H, Lee H, Jahng K. An improved hydrophilicity via electrospinning for enhanced cell attachment and proliferation. J Biomedical Mater Res Part B: Appl Biomater. 2005;78:283–90.
29. Wang J, Bei J, Wang S. Improving cell affinity of poly (D, L-lactide) film modified by anhydrous ammonia plasma treatment. Polym Adv Technol. 2002;13:220–6.
30. Anderson HC, Sipe JB, Hessle L, Dhanyamraju R, Atti E, Camacho NP, et al. Impaired calcification around matrix vesicles of growth plate and bone in alkaline phosphatase-deficient mice. Am J Pathol. 2004;164:841–7.
31. Jaiswal N, Haynesworth SE, Caplan AI, Bruder SP. Osteogenic differentiation of purified, culture-expanded human mesenchymal stem cells in vitro. J Cell Biochem. 1997;64:295–312.
32. Schaap-Oziemlak A, Raymakers RA, Bergevoet SM, Gilissen C, Jansen BJ, Adema GJ, et al. MicroRNA hsa-miR-135b regulates mineralization in osteogenic differentiation of human unrestricted somatic stem Cells (USSCs). Stem Cells Dev. 2010;19:877–85.
33. Halvorsen YD, Franklin D, Bond AL, Hitt DC, Auchter C, Boskey AL, et al. Extracellular matrix mineralization and osteoblast gene expression by human adipose tissue-derived stromal cells. Tissue Eng. 2001;7:729–41.
34. Zur Nieden NI, Kempka G, Ahr HJ. In vitro differentiation of embryonic stem cells into mineralized osteoblasts. Differentiation. 2003;71:18–27.
35. Khurana JS, McCarthy EF, Zhang PJ, Safadi FF. Bone Structure, Development and bone biology. Essentials in bone and soft-tissue Pathology. US: Springer; 2010. p. 1–15.
36. Handschel J, Naujoks C, Langenbach F, Berr K, Depprich R, Ommerborn M, et al. Comparison of ectopic bone formation of embryonic stem cells and cord blood stem cells in vivo. Tissue Eng Part A. 2010;16:2475–83.
37. Naujoks C, Langenbach F, Berr K, Depprich R, Kubler N, Meyer U, et al. Biocompatibility of osteogenic predifferentiated human cord blood stem cells with biomaterials and the influence of the biomaterial on the process of differentiation. J Biomater Appl. 2010. doi:10.1177/0885328209358631.
38. Aubin J, Triffitt J. Mesenchymal stem cells and osteoblast differentiation. Princ Bone Biol. 2002;1:59–81.
39. Guillot PV, De Bari C, Dell'Accio F, Kurata H, Polak J, Fisk NM. Comparative osteogenic transcription profiling of various fetal and adult mesenchymal stem cell sources. Differentiation. 2008;76:946–57.
40. Termine J, Kleinman H, Whitson S, Conn K, McGarvey M, Martin G. Osteonectin, a bone-specific protein linking mineral to collagen. Cell. 1981;26:99–105.
41. Wozney JM. The bone morphogenetic protein family and osteogenesis. Mol Reprod Dev. 1992;32:160–7.
42. Hauschka P, Lian J, Cole D, Gundberg C. Osteocalcin and matrix Gla protein: vitamin K-dependent proteins in bone. Physiol Rev. 1989;69:990.
43. Viereck V, Siggelkow H, Tauber S, Raddatz D, Schutze N, Hufner M. Differential regulation of Cbfa1/Runx2 and osteocalcin gene expression by vitamin-D3, dexamethasone, and local growth factors in primary human osteoblasts. J Cell Biochem. 2002;86:34.